Discriminating chaotic and stochastic dynamics through the permutation spectrum test

C. W. Kulp and L. Zunino

Citation: Chaos: An Interdisciplinary Journal of Nonlinear Science **24**, 033116 (2014); doi: 10.1063/1.4891179
View online: http://dx.doi.org/10.1063/1.4891179
View Table of Contents: http://scitation.aip.org/content/aip/journal/chaos/24/3?ver=pdfcov
Published by the AIP Publishing

Discriminating chaotic and stochastic dynamics through the permutation spectrum test

C. W. Kulp[1,a)] and L. Zunino[2,3,b)]
[1]*Department of Astronomy and Physics, Lycoming College, Williamsport, Pennsylvania 17701, USA*
[2]*Centro de Investigaciones Ópticas (CONICET La Plata—CIC), C.C. 3, 1897 Gonnet, Argentina*
[3]*Departamento de Ciencias Básicas, Facultad de Ingeniería, Universidad Nacional de La Plata (UNLP), 1900 La Plata, Argentina*

(Received 9 May 2014; accepted 14 July 2014; published online 23 July 2014)

In this paper, we propose a new heuristic symbolic tool for unveiling chaotic and stochastic dynamics: the *permutation spectrum test*. Several numerical examples allow us to confirm the usefulness of the introduced methodology. Indeed, we show that it is robust in situations in which other techniques fail (intermittent chaos, hyperchaotic dynamics, stochastic linear and nonlinear correlated dynamics, and deterministic non-chaotic noise-driven dynamics). We illustrate the applicability and reliability of this pragmatic method by examining real complex time series from diverse scientific fields. Taking into account that the proposed test has the advantages of being conceptually simple and computationally fast, we think that it can be of practical utility as an alternative test for determinism. © *2014 AIP Publishing LLC*. [http://dx.doi.org/10.1063/1.4891179]

The importance of distinguishing between periodic, chaotic, and stochastic dynamics from time series analysis is well-recognized for understanding the mechanisms that govern the regarded complex systems. In this work, we have introduced a conceptually simple and computationally fast symbolic visual test for discriminating chaotic and stochastic dynamics, called the permutation spectrum test. Because the symbolization is made by implementing the Bandt and Pompe methodology, all the advantages associated with this natural encoding (simplicity, extremely fast calculation, robustness, and invariance with respect to monotonous transformations) are inherited by the permutation spectrum test. We have shown that this pragmatic approach is robust in situations in which other tests fail. We have also confirmed its practical utility by examining several experimental and natural time series.

I. INTRODUCTION

It is widely accepted that identifying chaos from time series data is a very relevant problem for understanding, modeling, and forecasting purposes. Chaotic dynamics are deterministic, and hence predictable, albeit on short time scales. However, the accurate discrimination between low-dimensional chaotic and stochastic dynamics is regarded as one of the most challenging issues in nonlinear time series analysis. Essentially, the main difficulty lies in the fact that both, stochastic and chaotic processes, share many features.[1] A lot of effort has been done to try to shed some light on this critical and elusive problem. Without being exhaustive, we mention the correlation dimension,[2] Kolmogorov entropy,[3] Lyapunov exponents,[4] nonlinear predictive models,[5,6] determinism test,[7] "noise titration" technique,[8] and 0–1 test.[9] Nevertheless, none of these measures and tests are fully reliable and all of them suffer from severe limitations.[10–16] Moreover, experimental chaotic signals are unavoidably contaminated by noise, making the classification task even more difficult. These drawbacks motivate the search of new methods that can efficiently distinguish chaotic from stochastic time series.[17]

In this paper, we present a conceptually simple and computationally fast symbolic tool for unveiling the intrinsic dynamics of a system from which a time series has been measured. More precisely, we estimate the symbolic spectrum, originally suggested fifteen years ago by Yang and Zhao[18] and very recently took up again by Kulp and Smith,[19] but using the Bandt and Pompe (BP) symbolization scheme.[20] With this change, all the advantages associated with the BP recipe, namely, simplicity, extremely fast calculation, robustness, and invariance with respect to monotonous transformations are directly inherited. The proposed symbolic approach, hereafter called the *permutation spectrum test* (PST), allows us to distinguish between regular, chaotic, and stochastic dynamics from complex time series. Furthermore, it can be easily applied to the time series obtained from a representative variable of the complex system under analysis. Several conventional numerical simulation systems were analyzed in order to check the performance of the introduced approach on systems with known dynamics. We have found that reliable results are obtained in situations in which other methodologies fail. We have further illustrated the applicability of the PST characterizing the underlying dynamics associated with several experimental and natural time series. It is worth emphasizing here that the proposed heuristic approach is not introduced for replacing any of the presently available techniques. On the contrary, it is proposed to complement the information provided by them.

In the remainder of this work, we first describe our PST algorithm, then we apply this approach to several time series generated from model systems with known dynamics in

a)Kulp@lycoming.edu
b)lucianoz@ciop.unlp.edu.ar

order to confirm its effectiveness. Next, the test is applied to several real-world data sets with well-understood dynamical behavior. Finally, some concluding remarks are included.

II. PERMUTATION SPECTRUM TEST

The symbol spectrum test, developed by Yang and Zhao,[18] was proposed for distinguishing deterministic from stochastic dynamics. It begins by partitioning the original binary-symbolized time series into disjoint subsets of a particular length l. After that the symbol spectrum, i.e. the frequency of "words" at a particular level L of the symbol tree, is estimated for each partition. To estimate the symbol spectrum for each partition for a chosen L–value, the elements of the partition are grouped into "words" of length L. It was shown that the symbol spectra for the different partitions corresponding to deterministic signals preserve its form while those associated with stochastic time series do not have a definite shape. Summarizing, the symbol spectrum test is based on the repeatability of the frequency of "words" considered in the symbolization for shorter disjoint segments of the original records. The symbol spectra for the different partitions are plotted on the same graph and the degree of overlap is visually detected. The degree of overlap is used for classifying the type of dynamics. Please see Ref. 19 for further details about this methodology.

In this work, we introduce two modifications to the original symbol spectrum test. First, the encoding scheme due to BP[20] is implemented instead of the binary alphabet. It is well-known that this very simple and fast symbolic approach,[21] based on the ordinal relation between the amplitude of neighboring values, naturally arises from the time series, and allows one to avoid amplitude threshold dependencies that affect more conventional methods based on range partitioning.[22] This dynamic, difference-based symbolization,[23] as opposed to most of those in current practice, takes into account the causal information that stems from the temporal structure of the time series. Moreover, the ordinal pattern distribution is robust to noise and invariant with respect to any monotonous transformations. These properties are highly appreciated for the analysis of experimental data. Information-theory derived quantifiers estimated by implementing this ordinal pattern probability distribution have been successfully used in a wide range of applications; see, e.g., Ref. 24 and references therein. Furthermore, several ordinal-related tools have been proposed for the discrimination of chaotic and stochastic dynamics.[1,25–30]

Here, we will illustrate how to create ordinal patterns from the time series data. After the time series has been partitioned into disjoint windows of length l, as done in the Yang and Zhao test, two parameters, the embedding dimension $D > 1$ ($D \in \mathbb{N}$, number of symbols that form the ordinal pattern) and the embedding delay τ ($\tau \in \mathbb{N}$, time separation between symbols) are chosen. Guidelines for choosing D and τ will be discussed momentarily. Next, each window is further partitioned into subsets of length D with delay τ similar to phase space reconstruction by means of time-delay-embedding. The elements in each new partition (of length D) are replaced by their rank in the subset. For example, the partition with $D = 4$ given by $\{1.2, 7.8, 2.3, 1.0\}$ would become $\{2, 4, 3, 1\}$. Furthermore, each permutation of $\{1, 2, 3, 4\}$ could be assigned a value called the ordinal pattern index, or more simply, ordinal pattern. To continue our example, the ordinal pattern $\{2, 4, 3, 1\}$ could be assigned the value 12. Finally, the probability distribution of the ordinal patterns for each window of length l can be estimated and then plotted on the same graph, similar to the Yang and Zhao test. Figure 1 shows all possible ordinal patterns for $D = 4$. Taking into account that there are $D!$ potential permutations for a D-dimensional vector, the condition $l \gg D!$ must be satisfied in order to obtain a reliable estimation of the spectrum.[31] For practical purposes, BP suggest in their cornerstone paper[20] to estimate the frequency of ordinal patterns with $3 \leq D \leq 7$ and time lag $\tau = 1$ (consecutive points). Nevertheless, other values of $\tau > 1$ (non-consecutive points) might provide additional relevant information as has been recently shown.[30,32,33] By changing the value of the embedding delay τ different time scales are being considered.[34] It is worth noticing that τ physically corresponds to multiples of the sampling time of the signal under analysis. For further details about the BP methodology, we strongly recommend Ref. 33, where the construction principle of ordinal patterns and all possible orderings (patterns) for different embedding dimensions are clearly illustrated.

The second modification we propose for improving the symbol spectrum test is the estimation of the standard deviation of the frequency of each ordinal pattern for the different disjoint subsets of length l. The standard deviation of the spectra as a function of ordinal pattern is a more objective quantifier of the degree of overlap among the spectra than visual inspection alone. Thus, the *permutation spectrum test* analyzes the variability, via the standard deviation, of the spectrum of ordinal patterns for different disjoint segments of the time series. The term *permutation* refers to the fact that the symbolization is accomplished following the BP scheme.

III. NUMERICAL SIMULATIONS

In this section, the PST is demonstrated on time series generated by several model systems, both deterministic and stochastic, which cover a broad range of dynamical behaviors. The systems studied are the logistic map with various parameter values, uniformly distributed random numbers, fractional Brownian motion, the generalized Hénon map, stochastic nonlinear correlated dynamics, and a noise-driven sine map. In each case (except the noise-driven sine map, see below), time series of length $N = 200\,000$ data points were generated from each system. The PST was applied to those systems with a window length of $l = 1000$ data points, an embedding dimension $D = 4$ and an embedding delay $\tau = 1$. Similar results (not shown) were obtained for $D = 5$ and $\tau = 1$. Parameters were chosen considering the results obtained in Ref. 35: for discrete models higher D-values and $\tau = 1$ lead to clearer distinction between different dynamical regimes. Ordinal patterns were indexed following the same convention used by Parlitz *et al.* (please see Fig. 2 of Ref. 33). Although we check the PST on long time series, the

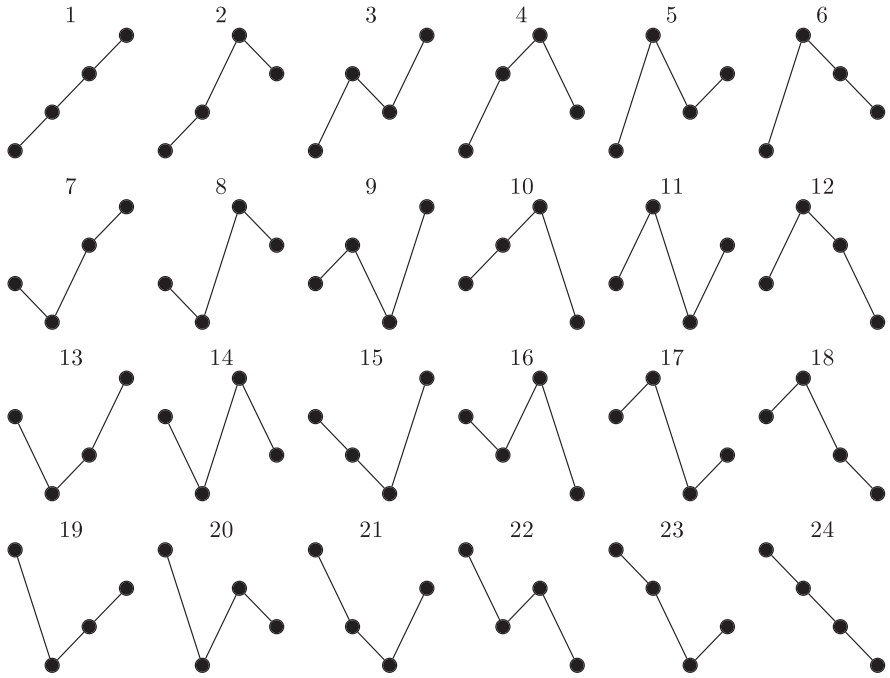

FIG. 1. The 24 possible outcomes for ordinal patterns with embedding dimension $D=4$. Ordinal patterns are numbered following the convention used by Parlitz *et al.*[33]

PST can also be applied to shorter time series as well. In the case of shorter time series, instead of partitioning the series into non-overlapping windows, one chooses a random element from a series. That random element would serve as the first element of the window from which the permutation spectrum can be found. Next, one would choose another (different) random element from the series, create the window, and find the permutation spectrum. This process can be repeated for as many windows as one wishes to use. Examples of using this overlapped implementation of the PST are presented in Sec. IV, where shorter experimental and natural records are analyzed. On the other hand, it is worth mentioning here that the window length l should be chosen in such a way that the overall dynamics of the systems under analysis will be included in each one of the overlapping or non-overlapping segments, e.g., in the case of a periodic signals several periods should be covered in each window.

We begin with a basic test for the PST, distinguishing between periodic, chaotic, and stochastic dynamics. Figure 2 shows the results of the PST when applied to time series generated by the logistic map, $x_{k+1}=rx_k(1-x_k)$, and uniformly distributed random numbers. Figure 2, like all of the next figures (except Figs. 5, 8, and 9) in this paper, consists of three rows, a short sample of the time series (top row), the permutation spectra (middle row), and the standard deviation of the spectra (bottom row). The left column of Fig. 2 shows the results of the PST applied to the logistic map with periodic dynamics, $r=3.55$. Because the dynamics is periodic, the same ordinal patterns repeat in the time series, hence there is no variation in the permutation spectra. The lack of variation can be seen in the graph of the permutation spectrum (middle row), where all 200 of the spectra lie on top of one another. Furthermore, this lack of variation results in a zero standard deviation for the spectra. The middle column of Fig. 2 shows the results of the PST applied to the logistic map with chaotic dynamics, $r=3.91$. Notice that there is more variation among the spectra as compared to the periodic case, illustrated by less overlap between the spectra and non-zero standard deviations for some ordinal patterns. The peak of each spectrum occurs at the same ordinal patterns, but the height of each peak varies from one window to the next. The variations in peak height for each ordinal pattern demonstrate that the dynamics is not periodic. However, the fact that the same ordinal patterns appear in each spectra show that the system is deterministic. Notice that there are some "forbidden patterns,"[25,26,28] ordinal patterns that do not occur in the spectra. These forbidden ordinal patterns are not produced by the mathematical rules (in this case, the logistic map) that govern the system. Forbidden patterns have been successfully applied to a wide range of problems, such as to demonstrate evidence of deterministic dynamics during epileptic states[36,37] and to quantify the degree of market inefficiency.[38] The forbidden patterns are obviously consistent from one spectrum to the next, as shown by the zero standard deviation of those patterns. This is in contrast to the uniformly distributed uncorrelated noise whose results are presented in the right column of Fig. 2. Notice that like the chaotic dynamics, there is variation between the spectra. However, unlike the chaotic dynamics, there are no consistently forbidden patterns in the spectra. All ordinal patterns appear, because the dynamics is random. As will be seen in later examples, it is the presence of consistently forbidden ordinal patterns, ordinal patterns that do not appear in the spectra and have zero standard deviation, that distinguishes deterministic from stochastic dynamics.

Figure 3 illustrates the results of the PST applied to fractional Brownian motion (fBm) with various Hurst exponents,

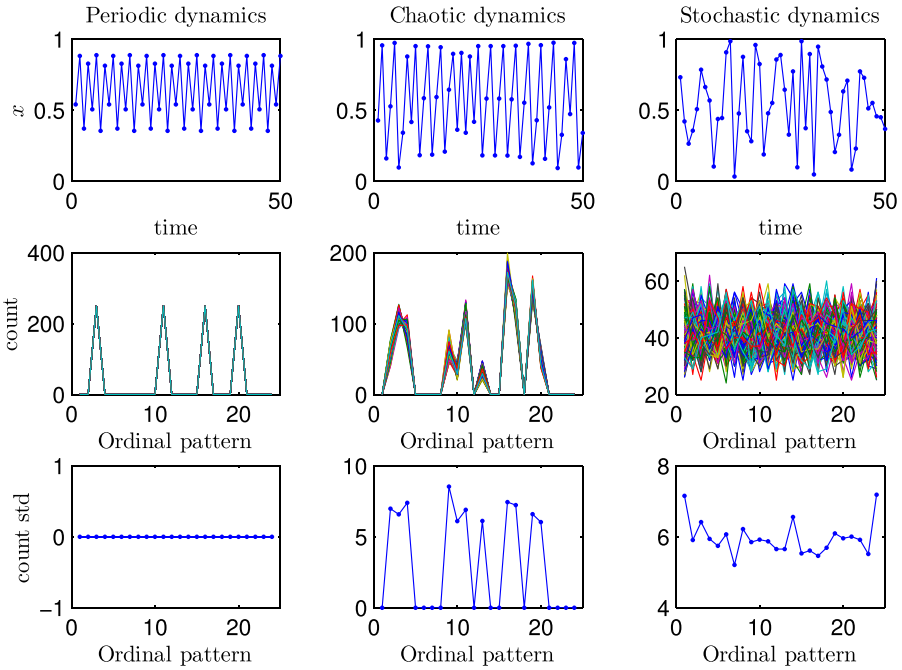

FIG. 2. Short sample of the time series (top row), permutation spectra (middle row), and standard deviation of the spectra (bottom row) for numerical realizations of the logistic map with periodic ($r = 3.55$) and chaotic dynamics ($r = 3.91$) in the left and middle columns, respectively, and for an uniformly distributed noise in the right column. Two hundred permutation spectra for the different disjoint subsets of length $l = 1000$ data points were plotted (middle row). $D = 4$ and $\tau = 1$ were chosen for the BP symbolization recipe.

H. Applying the PST to fBm gives the opportunity to see how well the PST handles linearly correlated stochastic processes, traditionally a difficult case for tests for determinism.[10,11,14] Figure 3 shows that the PST can successfully determine the stochasticity of each time series. Although in Fig. 3 the permutation spectra appear to be similar to those of a chaotic series, the standard deviation clearly shows no consistent forbidden patterns. Furthermore, the strong positive correlation for the $H = 0.7$ case appears in the permutation spectra with each spectrum having a peak at similar ordinal patterns (please compare with the PST for the fully uncorrelated stochastic process, right column of Fig. 2).

Figure 4 shows the results of the PST applied to the generalized Hénon map

$$x_{k+1} = a - (x_{k+2-n})^2 - b x_{k+1-n}, \tag{1}$$

where $n = 3$, $a = 1.76$, and $b = 0.1$.[39] The parameters chosen result in the generalized Hénon map displaying high-dimensional chaotic or hyperchaotic behavior in which there is more than one positive Lyapunov exponent. Note that in Ref. 39, Eq. (1) is shown to be a reduction of an n-dimensional map, hence it is possible to discuss multiple Lyapunov exponents for the system described by this equation. The permutation spectra have significant amounts of variation for almost all of the ordinal patterns. However, there are some, albeit very few, consistently forbidden patterns, as shown by the standard deviation. The presence of consistently forbidden patterns shows that the dynamics is deterministic. The small

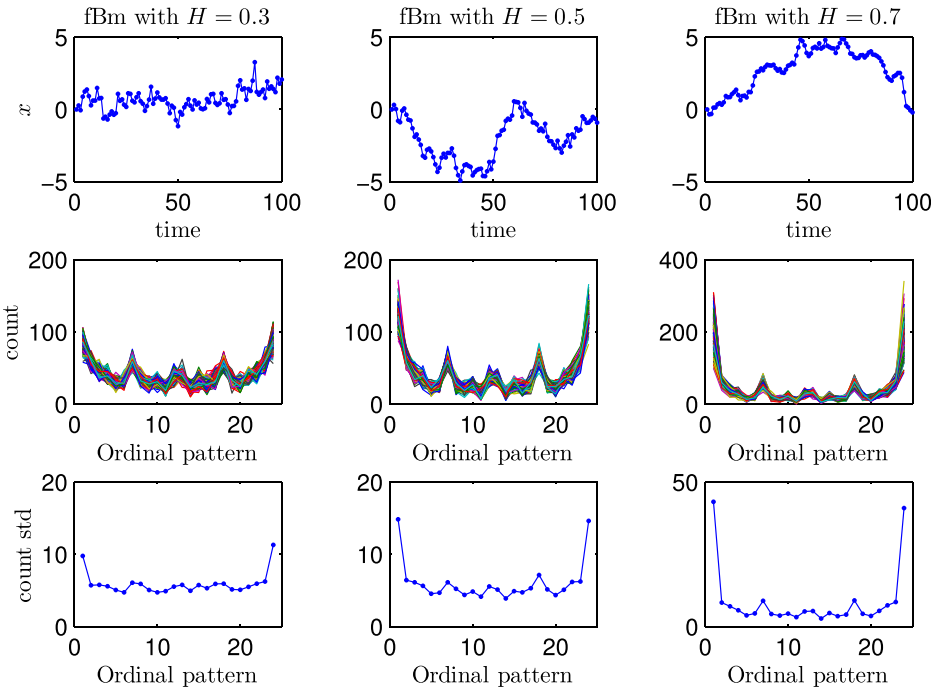

FIG. 3. Short sample of the time series (top row), permutation spectra (middle row), and standard deviation of the spectra (bottom row) for numerical realizations of fBm with $H = 0.3$ (left column), $H = 0.5$ (middle column), and $H = 0.7$ (right column). Two hundred permutation spectra for the different disjoint subsets of length $l = 1000$ data points were plotted (middle row). $D = 4$ and $\tau = 1$ were chosen for the BP symbolization recipe.

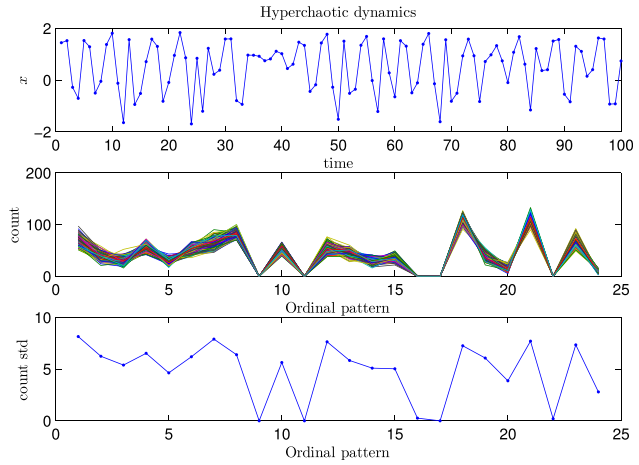

FIG. 4. Short sample of the time series (top row), permutation spectra (middle row), and standard deviation of the spectra (bottom row) for numerical realizations of the generalized Hénon map displaying hyperchaotic behavior. Two hundred permutation spectra for the different disjoint subsets of length $l = 1000$ data points were plotted (middle row). $D = 4$ and $\tau = 1$ were chosen for the BP symbolization recipe.

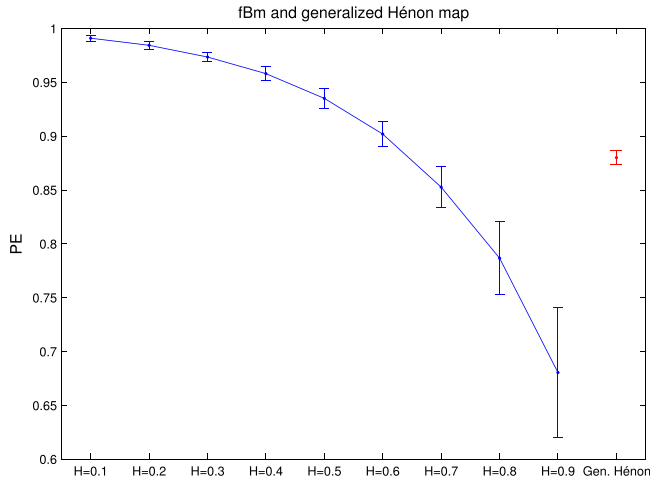

FIG. 5. Estimated PE values, with $D = 4$ and $\tau = 1$, for fBm with Hurst $H \in \{0.1, 0.2, ...0.9\}$ (blue) and the generalized Hénon map (red). Mean and standard deviation of the PE values obtained for the two hundreds disjoint windows of length $l = 1000$ are plotted.

number of forbidden patterns is a hallmark of the hyperchaotic behavior. Hence, the PST is able to distinguish high-dimensional chaos from stochastic behavior. Furthermore, this result shows that, in principle, the PST could also distinguish between hyperchaotic and chaotic dynamics, although more work needs to be done in this area.

Before moving on to other model series, we can compare the results of the PST to a well-known global-permutation-information theoretic quantifier typically used for characterizing regular, chaotic, and random behavior, the permutation entropy (PE).[20,21] The PE is just the normalized Shannon entropy, $S[P] = -\sum_{i=1}^{D!} p_i \ln p_i / \ln D!$, evaluated using the ordinal pattern probability distribution $P = \{p_1, \ldots, p_{D!}\}$, where p_i represents the relative frequency of the ordinal pattern whose index is i. PE characterizes the diversity of the orderings present in the complex time series. As an example of how the PST compares to the PE, we estimate the mean and standard deviation of the PE for two hundred disjoint windows of length $l = 1000$ for the generalized Hénon map and for fBm with Hurst exponents $H \in \{0.1, 0.2, ...0.9\}$. The results are plotted in Fig. 5. Because the PE result for the generalized Hénon map falls with in the range of PE's for fBm with $H > 0.5$, we can see that the PE is not able to distinguish the hyperchaotic dynamics of the generalized Hénon map from persistent correlated stochastic processes. We believe that a further study comparing the PST to the PE would be a valuable avenue for future research.

Figure 6 shows the results of the PST applied to an intermittent chaotic system: the logistic map with $r = 3.8284$.[16] Intermittent chaotic dynamics are shown by systems that display chaotic behavior for short periods of time between longer periods of regular behavior. This behavior is illustrated in the top plot of Fig. 6, where long periods of periodicity are interrupted by short periods of chaos. As mentioned in Ref. 16, traditional methods for computing Lyapunov exponents, based on global average, fail in intermittent chaotic systems since the laminar phase dominates. The PST, however, is able to detect the chaotic behavior. Notice in Fig. 6, the permutation spectra have some variation, unlike a periodic system. Furthermore, there are clear consistent forbidden ordinal patterns. Both the permutation spectra and the standard deviation are more similar to the chaotic logistic map results in Fig. 2 than the periodic logistic map results.

Another case that is difficult for many tests for determinism is stochastic nonlinear correlated dynamics. An example of such a system is

$$x_{k+1} = a\nu_k + b\nu_{k-1}(1 - \nu_k), \tag{2}$$

where ν_k is a uniform independently and identically distributed (iid) random variable with values between 0 and 1, $a = 3$ and $b = 4$.[15,16] A discussion about the stochasticity of Eq. (2) is found in Ref. 15. Figure 7 shows the results of the PST applied to this system. Notice that each spectrum has a peak at similar ordinal patterns, a sign that the PST is detecting correlations in the data, similar to the fBm case. However, there are no consistently forbidden ordinal patterns. Hence, the PST successfully detects the stochasticity

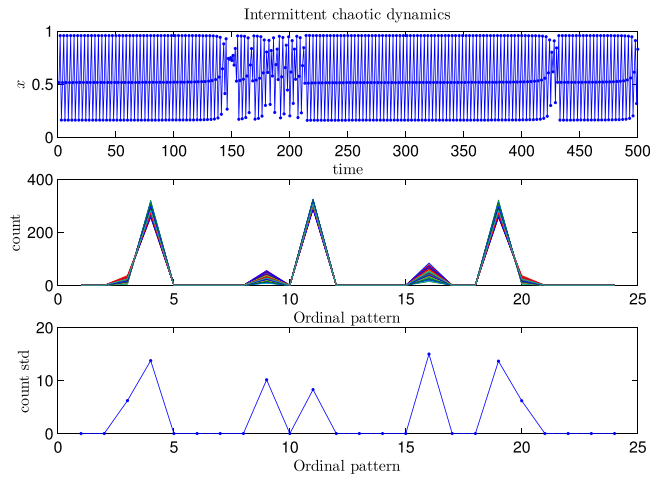

FIG. 6. Same as Fig. 4 but for an intermittent chaotic dynamics.

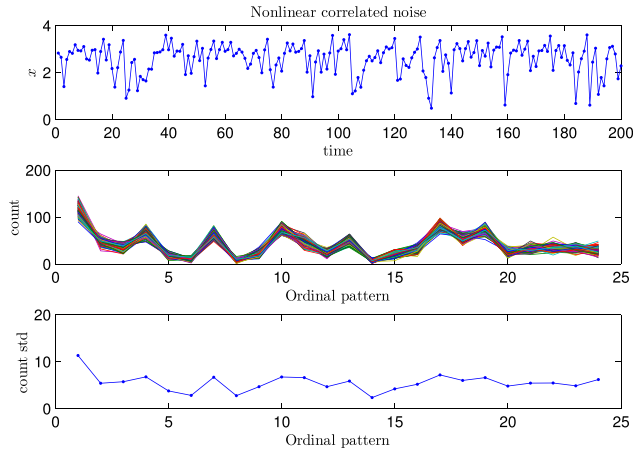

FIG. 7. Same as Fig. 4 but for a stochastic nonlinear correlated dynamics.

of the system. It is worth remarking here that the "noise titration" technique fails to distinguish this non-chaotic signal.[15,16]

The final model system studied is the noise-driven sine map

$$x_{k+1} = \mu \sin(x_k) + Y_k \eta_k, \tag{3}$$

where, as described in Ref. 15, μ is the map parameter, η_k is an iid random variable with a uniform distribution between $-b$ and b, and Y_k is a random variable from a Bernoulli process. The variable Y_k takes on the value 1 with a probability of q and a value of 0 with a probability of $1-q$. The value of q serves as a measure of the amount of dynamical noise; when q is small, noise perturbations are very rare. In Refs. 15 and 16, it was shown that the "noise titration" technique incorrectly characterizes this system as chaotic for $\mu = 2.4$, $b = 2$, and $q = 0.01$. Figure 8 shows the result of the PST applied to numerical realizations of Eq. (3) with the same parameter values used in Refs. 15 and 16. Notice that the standard deviation, while small is never zero. This illustrates the presence of a small amount of noise in the system. The symbol spectra, however, suggest that the system has some periodicity due to the presence of a few distinct peaks. Those

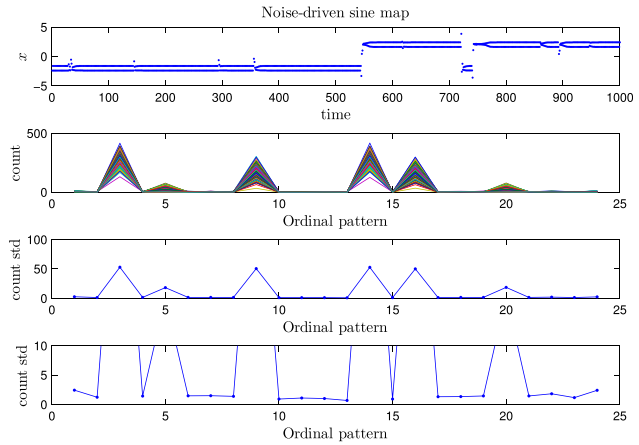

FIG. 8. Same as Fig. 4 but for the noise-driven sine map. The bottom plot shows an enlargement of the region with low standard deviation of the spectra for a better visualization.

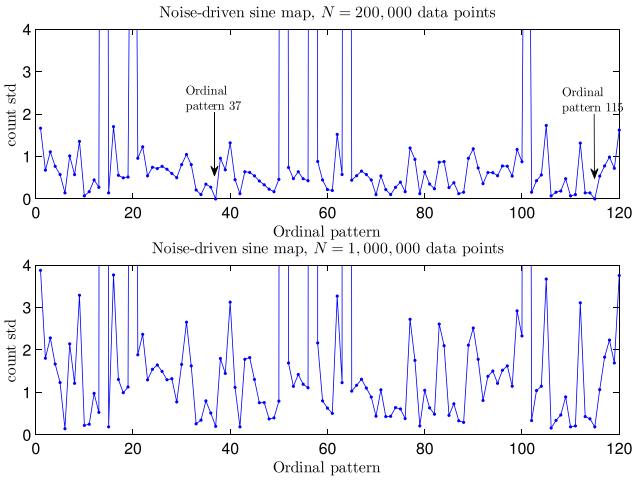

FIG. 9. Standard deviation of the permutation spectra for the noise-driven sine map estimated with $D = 5$ and $\tau = 1$. Numerical realizations of lengths $N = 200\,000$ and $N = 1\,000\,000$ data points were analyzed by using 200 windows of $l = 1000$ (top row) and 200 windows of $l = 5000$ (bottom row). Note the presence of two missing patterns (ordinal patterns 37 and 115) in the analysis of the shorter time series.

peaks have significant variations in height (due to the noise), but appear similar to the periodic logistic map results in Fig. 2. This is different from the intermittent chaos case, because unlike intermittent chaos, the noise-driven sine map has no consistently forbidden ordinal patterns. Hence, the PST shows that Eq. (3) is a noisy periodic system. It should also be noted that for this example, longer time series were needed to illustrate the fact that there are no forbidden patterns when an encoding with embedding dimension $D = 5$ is implemented. More precisely, 200 windows of $l = 5000$ elements were used, for a total time series of $N = 1\,000\,000$ data points. The first time the PST was applied to this system, 200 windows of $l = 1000$ elements were used and two apparently forbidden patterns appeared for the PST with $D = 5$ as it can be seen in the top plot of Fig. 9. The test was ran again with the longer time series and it was found that those patterns which were initially thought to be forbidden, in fact, were simply *missing*[40] from the shorter time series (bottom plot of Fig. 9). It should be emphasized that for $D = 4$, the false forbidden patterns did not occur in the noise-driven sine map. Furthermore, all of the systems studied in this section were examined with both $D = 4$ and $D = 5$, although the results for $D = 5$ are not shown for most of the systems. The noise-driven sine map was the only numerical system studied that demonstrated sensitivity to the length of the time series used in the PST with $D = 5$.

According to the findings obtained with the numerical analysis performed in this section, the following decision rules can be concluded: (i) if no forbidden patterns are detected, the system is stochastic; (ii) permutation spectrum with a zero standard deviation suggests that the dynamics is periodic; and (iii) chaotic dynamics will have some forbidden patterns and a non-zero standard deviation for some patterns. Our results also indicate that hyperchaotic dynamics have fewer forbidden patterns. However, using forbidden patterns to discriminate between chaotic and hyperchaotic dynamics is an avenue of future research.

IV. REAL-WORLD APPLICATIONS

In this section, we apply the PST to real-world time series with well-understood dynamics from several scientific fields. The main intention is to illustrate its applicability and reliability in practical contexts. For this purpose, we have analyzed the performance of the PST for characterizing complex time series derived from an experimental chaotic laser, a geophysical process (North Atlantic oscillation (NAO)) and the historical price evolution described by two commodities (crude oil and gold). In order to overcome the analysis of these short time series, we have estimated the permutation spectrum for overlapping segments of length l. More precisely, 1000 different subsets randomly chosen from the original time series data were taken into consideration. The degree of overlap of the permutation spectra for these 1000 subseries was employed to conclude in favor of a stochastic or a chaotic dynamics.

As a first experimental example, we have analyzed the longer data set ($N = 9093$ data points) of laser chaotic intensity pulsations included in the Santa Fe Time Series Competition (series A from Ref. 41). For further details about this experimental record please see Ref. 42. Briefly, chaotic intensity pulsations of an unidirectional far-infrared NH_3 ring laser at 81.5 μm were recorded with an oscilloscope. Signatures of an underlying chaotic dynamics is directly concluded from the analysis performed with the PST by estimating the permutation spectra for 1000 different randomly selected subsets of length $l = 1000$ data points with $D = 4$ and $\tau = 1$ (Fig. 10). A similar conclusion is derived by implementing the PST with $D = 5$ and $\tau = 1$ (not shown).

As a second practical example, the NAO index, calculated as the difference between the normalized sea level pressure at two action centres, the southernmost one located at the Azores High and the northernmost at the Icelandic Low,[43] was characterized through the PST. The NAO is an atmospheric spatio-temporal phenomenon observed over the North Atlantic Ocean, with significant influence on the winter weather over Western and Central Europe. Since large changes in surface temperature and precipitation in this region are strongly influenced by the NAO, there is a particular interest to unveil the underlying nature of its dynamics. The fluctuations of the NAO phenomenon are quantified through the NAO index. The monthly mean NAO index from January 1950 to January 2014 ($N = 769$ data points), downloaded from the Climate Prediction Center website,[44] was examined. Results obtained for this geophysical processes are depicted in Fig. 11. For this very short record, the study was performed estimating the permutation spectra for 400 different randomly selected subsets of length $l = 200$ data points with $D = 4$ and $\tau = 1$. The PST concludes in favor of a stochastic dynamics for modeling this climatic index in agreement with the finding obtained by other authors.[43,45–49]

Finally, as the third and last real-world application, we have studied the historical temporal daily price evolution of two relevant commodities, namely, crude oil and gold. The former is the major energy source for the present economic activity, and the latter one is extremely popular for investment purposes. For these reasons, it is significant to try to shed some light on the nature of their dynamics. More precisely, we have analyzed the daily closing spot price of the West Texas Intermediate (WTI) from January 2nd, 1986 to December 31st, 2013 ($N = 7162$ oil price observations) obtained from the U.S. Energy Information Administration (EIA) website[50] (quoted in U.S. dollars per barrel), and the daily gold price from January 2nd, 1973 to December 31st, 2013 ($N = 10205$ gold price observations) extracted from the USAGOLD website[51] (quoted in U.S. dollars per ounce). Figures 12 and 13 show the results obtained. In both cases, 1000 different randomly selected subsets of length $l = 1000$ data points, $D = 4$ and $\tau = 1$ were employed in the analysis (similar results were obtained by using $D = 5$ and $\tau = 1$). According to the PST, the dynamics of both commodities appear to be consistent with a stochastic explanation. On the one hand, the stochastic behavior found for the crude oil prices is supported by the recent characterization performed by Barkoulas *et al.*[52] implementing more conventional diagnostic tools (correlation dimension, Lyapunov exponents, and

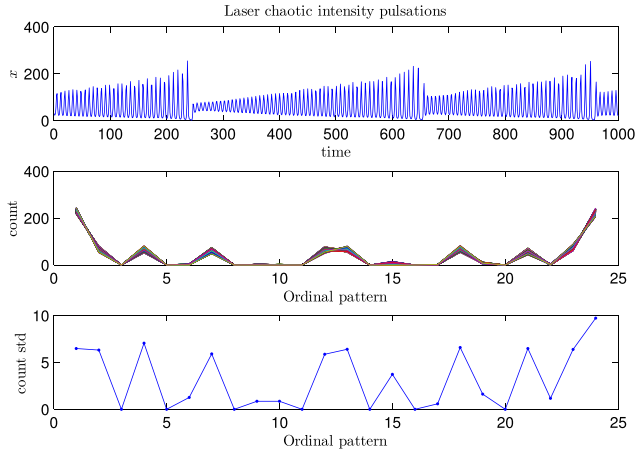

FIG. 10. Short sample of the time series (top row), permutation spectra (middle row), and standard deviation of the spectra (bottom row) for laser chaotic experimentally generated data. Permutation spectra with $D = 4$ and $\tau = 1$ for 1000 different randomly selected subsets of length $l = 1000$ data points were plotted (middle row).

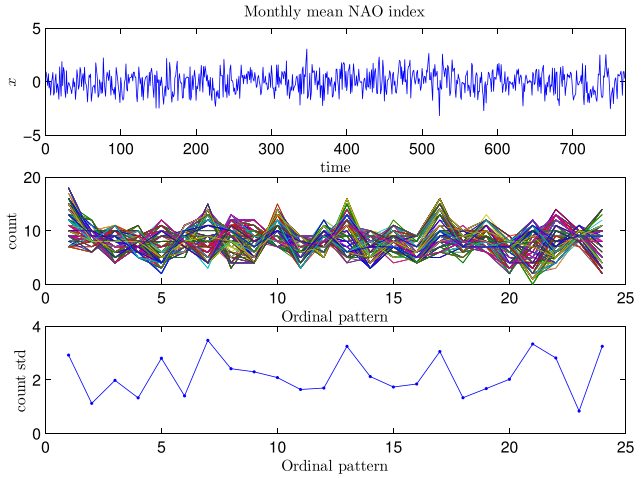

FIG. 11. Time series (top row), permutation spectra (middle row), and standard deviation of the spectra (bottom row) for the monthly mean NAO index. Permutation spectra with $D = 4$ and $\tau = 1$ for 400 different randomly selected subsets of length $l = 200$ data points were plotted (middle row).

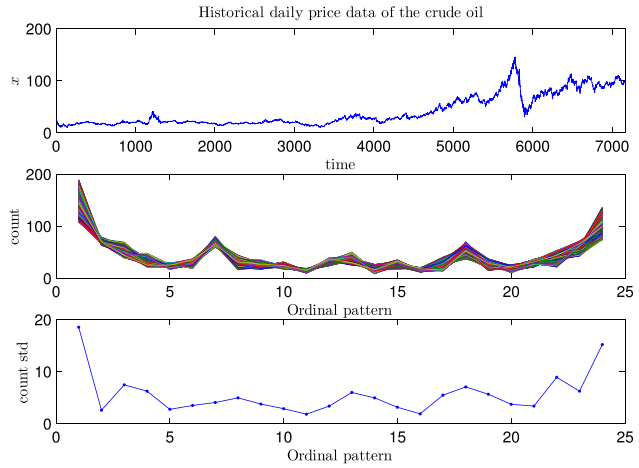

FIG. 12. Time series (top row), permutation spectra (middle row), and standard deviation of the spectra (bottom row) for the historical daily price data of the crude oil. Permutation spectra with $D=4$ and $\tau=1$ for 1000 different randomly selected subsets of length $l=1000$ data points were plotted (middle row).

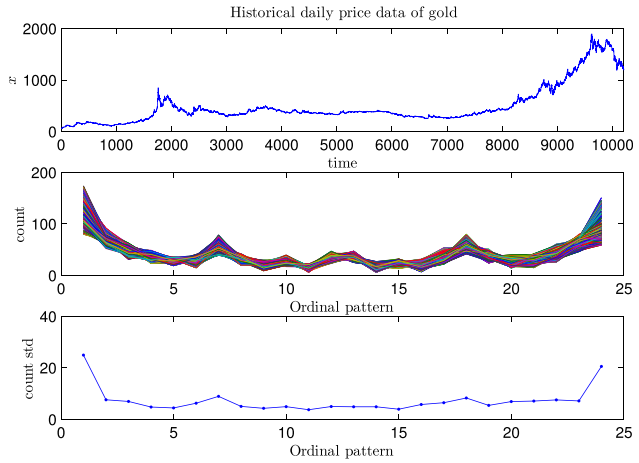

FIG. 13. Time series (top row), permutation spectra (middle row), and standard deviation of the spectra (bottom row) for the historical daily price data of gold. Permutation spectra with $D=4$ and $\tau=1$ for 1000 different randomly selected subsets of length $l=1000$ data points were plotted (middle row).

recurrence plots). On the other hand, the rejection of an intrinsic deterministic nature for the gold prices is against the evidence of a chaotic structure in the rates of return of gold and silver obtained by Frank and Stengos.[53] It is worth remarking here that the high correlation and cointegration confirmed between crude oil and gold markets[54] allows to conjecture that both commodities should share the same dynamics. The results we have obtained via the PST support this fact. By comparing Figs. 12 and 13, it is concluded that the permutation spectra look very similar.

V. CONCLUSIONS

We have introduced the permutation spectrum test, a new heuristic and pragmatic test for determinism which can also be potentially used for characterizing the dynamics of a system from time series data. The standard deviation of the permutation spectra is used to determine whether or not a time series is deterministic by detecting consistently forbidden ordinal patterns in the spectra. In our studies thus far, spectra that have a zero standard deviation represent periodic data, whereas spectra with some variation but several consistent forbidden patterns are hallmarks of chaotic data. Stochastic data have a non-zero standard deviation for all ordinal patterns, i.e., no patterns are forbidden. The PST correctly identifies the stochasticity of linearly and nonlinearly correlated noise, both are traditionally difficult cases for tests for determinism. Likewise, the PST can also successfully detect the determinism in other difficult cases such as hyperchaotic and intermittent chaotic dynamics. In one case, the noise-driven sine map, the PST was able to correctly characterize the system as noisy periodic dynamics. Finally, through the analysis of several real-world complex time series data its applicability and reliability in practical contexts were confirmed.

There are still several open avenues of research for the PST. First, how well does the PST handle data measured from continuous systems? This is essentially the question of how sampling rates affect the PST's ability to successfully characterize a time series. Second, how does irregular sampling affect the PST's ability to detect determinism? The ordinal patterns are created from consecutive elements of the series. What happens to the spectra when there are different amounts of time between the elements used to create the ordinal patterns? Finally, and perhaps most importantly, how robust is the PST to noise. The persistence of forbidden patterns in noisy deterministic data numerically confirmed by Amigó *et al.*[25] allows one to guess robustness of the PST in a noisy environment. We saw with the noise-driven sine map that the PST can successfully characterize periodic dynamics with low levels of dynamical noise. Can the PST be successfully applied to chaotic systems with low levels of noise? How well can the PST handle higher noise amounts? Can the PST be reliably used to distinguish between noisy deterministic data and purely stochastic data? All of these questions are beyond the scope of the present study, whose purpose was simply to introduce the PST. However, all of these questions will need to be carefully answered in order to reliably apply the PST to real-world data which is typically noisy and irregularly sampled.

ACKNOWLEDGMENTS

Luciano Zunino acknowledges Consejo Nacional de Investigaciones Científicas y Técnicas (CONICET), Argentina and Universidad Nacional de La Plata (UNLP), Argentina for their support. The authors would like to thank the two anonymous reviewers for their constructive comments.

[1]O. A. Rosso, H. A. Larrondo, M. T. Martín, A. Plastino, and M. A. Fuentes, "Distinguishing noise from chaos," Phys. Rev. Lett. **99**, 154102 (2007).
[2]P. Grassberger and I. Procaccia, "Measuring the strangeness of strange attractors," Physica D **9**, 189–208 (1983).
[3]P. Grassberger and I. Procaccia, "Estimation of the Kolmogorov entropy from a chaotic signal," Phys. Rev. A **28**, 2591–2593 (1983).
[4]A. Wolf, J. B. Swift, H. L. Swinney, and J. A. Vastano, "Determining Lyapunov exponents from a time series," Physica D **16**, 285–317 (1985).

[5]M. Casdagli, "Nonlinear prediction of chaotic time series," Physica D **35**, 335–356 (1989).
[6]M. B. Kennel and S. Isabelle, "Method to distinguish possible chaos from colored noise and to determine embedding parameters," Phys. Rev. A **46**, 3111–3118 (1992).
[7]D. T. Kaplan and L. Glass, "Direct test for determinism in a time series," Phys. Rev. Lett. **68**, 427–430 (1992).
[8]C.-S. Poon and M. Barahona, "Titration of chaos with added noise," Proc. Natl. Acad. Sci. U. S. A. **98**, 7107–7112 (2001).
[9]G. A. Gottwald and I. Melbourne, "A new test for chaos in deterministic systems," Proc. R. Soc. London, Ser. A **460**, 603–611 (2004).
[10]A. R. Osborne and A. Provenzale, "Finite correlation dimension for stochastic systems with power-law spectra," Physica D **35**, 357–381 (1989).
[11]A. Provenzale, A. R. Osborne, and R. Soj, "Convergence of the k_2 entropy for random noises with power law spectra," Physica D **47**, 361–372 (1991).
[12]J.-P. Eckmann and D. Ruelle, "Fundamental limitations for estimating dimensions and Lyapunov exponents in dynamical systems," Physica D **56**, 185–187 (1992).
[13]M. Dämmig and F. Mitschke, "Estimation of Lyapunov exponents from time series: The stochastic case," Phys. Lett. A **178**, 385–394 (1993).
[14]J. Hu, W. W. Tung, J. Gao, and Y. Cao, "Reliability of the 0-1 test for chaos," Phys. Rev. E **72**, 056207 (2005).
[15]U. S. Freitas, C. Letellier, and L. A. Aguirre, "Failure in distinguishing colored noise from chaos using the "noise titration" technique," Phys. Rev. E **79**, 035201(R) (2009).
[16]J. Gao, J. Hu, X. Mao, and W. W. Tung, "Detecting low-dimensional chaos by the "noise titration" technique: Possible problems and remedies," Chaos, Solitons Fractals **45**, 213–223 (2012).
[17]L. Lacasa and R. Toral, "Description of stochastic and chaotic series using visibility graphs," Phys. Rev. E **82**, 036120 (2010).
[18]Z. Yang and G. Zhao, "Application of symbolic techniques in detecting determinism in time series," in *Proceedings of the 20th Annual International Conference of the IEEE Engineering in Medicine and Biology Society* (1998), Vol. 20, pp. 2670–2673.
[19]C. W. Kulp and S. Smith, "Characterization of noisy symbolic time series," Phys. Rev. E **83**, 026201 (2011).
[20]C. Bandt and B. Pompe, "Permutation entropy: A natural complexity measure for time series," Phys. Rev. Lett. **88**, 174102 (2002).
[21]Y. Cao, W. W. Tung, J. B. Gao, V. A. Protopopescu, and L. M. Hively, "Detecting dynamical changes in time series using the permutation entropy," Phys. Rev. E **70**, 046217 (2004).
[22]E. M. Bollt, T. Stanford, Y.-C. Lai, and K. Życzkowski, "Validity of threshold-crossing analysis of symbolic dynamics from chaotic time series," Phys. Rev. Lett. **85**, 3524–3527 (2000).
[23]C. S. Daw, C. E. A. Finney, and E. R. Tracy, "A review of symbolic analysis of experimental data," Rev. Sci. Instrum. **74**, 915–930 (2003).
[24]M. Zanin, L. Zunino, O. A. Rosso, and D. Papo, "Permutation entropy and its main biomedical and econophysics applications: A review," Entropy **14**, 1553–1577 (2012).
[25]J. M. Amigó, S. Zambrano, and M. A. F. Sanjuán, "True and false forbidden patterns in deterministic and random dynamics," Europhys. Lett. **79**, 50001 (2007).
[26]J. M. Amigó, S. Zambrano, and M. A. F. Sanjuán, "Combinatorial detection of determinism in noisy time series," Europhys. Lett. **83**, 60005 (2008).
[27]M. Zanin, "Forbidden patterns in financial time series," Chaos **18**, 013119 (2008).
[28]J. M. Amigó, S. Zambrano, and M. A. F. Sanjuán, "Detecting determinism in time series with ordinal patterns: A comparative study," Int. J. Bifurcation Chaos **20**, 2915–2924 (2010).
[29]M. Matilla-García and M. Ruiz Marín, "A new test for chaos and determinism based on symbolic dynamics," J. Econ. Behav. Organ. **76**, 600–614 (2010).
[30]L. Zunino, M. C. Soriano, and O. A. Rosso, "Distinguishing chaotic and stochastic dynamics from time series by using a multiscale symbolic approach," Phys. Rev. E **86**, 046210 (2012).
[31]M. Staniek and K. Lehnertz, "Parameter selection for permutation entropy measurements," Int. J. Bifurcation Chaos **17**, 3729–3733 (2007).
[32]L. Zunino, M. C. Soriano, I. Fischer, O. A. Rosso, and C. R. Mirasso, "Permutation-information-theory approach to unveil delay dynamics from time-series analysis," Phys. Rev. E **82**, 046212 (2010).
[33]U. Parlitz, S. Berg, S. Luther, A. Schirdewan, J. Kurths, and N. Wessel, "Classifying cardiac biosignals using ordinal pattern statistics and symbolic dynamics," Comput. Biol. Med. **42**, 319–327 (2012).
[34]C. Bandt, "Ordinal time series analysis," Ecol. Modell. **182**, 229–238 (2005).
[35]M. Riedl, A. Müller, and N. Wessel, "Practical considerations of permutation entropy," Eur. Phys. J. Spec. Top. **222**, 249–262 (2013).
[36]G. Ouyang, X. Li, C. Dang, and D. A. Richards, "Deterministic dynamics of neural activity during absence seizures in rats," Phys. Rev. E **79**, 041146 (2009).
[37]K. Schindler, H. Gast, L. Stieglitz, A. Stibal, M. Hauf, R. Wiest, L. Mariani, and C. Rummel, "Forbidden ordinal patterns of periictal intracranial EEG indicate deterministic dynamics in human epileptic seizures," Epilepsia **52**, 1771–1780 (2011).
[38]L. Zunino, M. Zanin, B. M. Tabak, D. G. Pérez, and O. A. Rosso, "Forbidden patterns, permutation entropy and stock market inefficiency," Physica A **388**, 2854–2864 (2009).
[39]H. Richter, "The generalized hénon maps: Examples for higher-dimensional chaos," Int. J. Bifurcation Chaos **12**, 1371–1384 (2002).
[40]L. C. Carpi, P. M. Saco, and O. A. Rosso, "Missing ordinal patterns in correlated noises," Physica A **389**, 2020–2029 (2010).
[41]See http://www-psych.stanford.edu/~andreas/Time-Series/SantaFe.html to download the experimental chaotic laser record.
[42]U. Hübner, N. B. Abraham, and C. O. Weiss, "Dimensions and entropies of chaotic intensity pulsations in a single-mode far-infrared NH_3 laser," Phys. Rev. A **40**, 6354–6365 (1989).
[43]I. Fernández, C. N. Hernández, and J. M. Pacheco, "Is the North Atlantic oscillation just a pink noise?" Physica A **323**, 705–714 (2003).
[44]See http://www.cpc.ncep.noaa.gov/ to download the monthly mean NAO index.
[45]D. B. Stephenson, V. Pavan, and R. Bojariu, "Is the North Atlantic oscillation a random walk?" Int. J. Climatol. **20**, 1–18 (2000).
[46]C. Collette and M. Ausloos, "Scaling analysis and evolution equation of the North Atlantic oscillation index fluctuations," Int. J. Mod. Phys. C **15**, 1353–1366 (2004).
[47]P. G. Lind, A. Mora, M. Haase, and J. A. C. Gallas, "Minimizing stochasticity in the NAO index," Int. J. Bifurcation Chaos **17**, 3461–3466 (2007).
[48]M. D. Martínez, X. Lana, A. Burgueño, and C. Serra, "Predictability of the monthly North Atlantic oscillation index based on fractal analyses and dynamic system theory," Nonlinear Processes Geophys. **17**, 93–101 (2010).
[49]I. Fernández, J. M. Pacheco, and M. P. Quintana, "Pinkness of the North Atlantic oscillation signal revisited," Physica A **389**, 5801–5807 (2010).
[50]See http://www.eia.gov/ to download the historical temporal daily price evolution of crude oil.
[51]See http://www.usagold.com/ to download the historical temporal daily price evolution of gold.
[52]J. T. Barkoulas, A. Chakraborty, and A. Ouandlous, "A metric and topological analysis of determinism in the crude oil spot market," Energy Econ. **34**, 584–591 (2012).
[53]M. Frank and T. Stengos, "Measuring the strangeness of gold and silver rates of return," Rev. Econ. Stud. **56**, 553–567 (1989).
[54]Y.-J. Zhang and Y.-M. Wei, "The crude oil market and the gold market: Evidence for cointegration, causality and price discovery," Resour. Policy **35**, 168–177 (2010).